International Journal of Electronics Communication and Computer Engineering
Volume 4, Issue 2, ISSN (Online): 2249–071X, ISSN (Print): 2278–4209

Residual Stress Evaluation in Butt Welded Joint of ASTM A36 Steel Plates

M. Jeyakumar
Deptt. of Mechanical Engg,
Sardar Raja College of Engineering,
Tamilnadu, India

T. Christopher
Deptt. of Mechanical Engg,
Government College of Engineering,
Tamilnadu, India

B. Nageswara Rao
Deptt. of Mechanical Engg,
KL University, Green Fields,
Vaddeswaram, India

***Abstract* — In this work thermo-mechanical 3D finite element analysis has been performed to assess the residual stresses in the butt-weld joints of ASTM A36 steel plates utilizing the commercial software package ANSYS. The finite element model is employed to evaluate transient temperature distribution and the residual stress fields during welding. The welding simulation was considered as a sequentially coupled thermo mechanical analysis. To make use of the advantage of geometrical symmetry, only one plate is considered for analysis. Temperature dependant properties of the material are specified. The spherical volume-specific density heat source distribution is considered with a radius r_b. Convective and radiative heat losses are taken into account through boundary conditions for the outward flux. The residual stress distribution and magnitude in all directions and equivalent stress are obtained. The present 3D analysis results are found to be in good agreement with experimental results and existing 2D finite element analysis.**

***Keywords* – ASTM A36 Steel, Butt-Weld, Convection and Radiation Heat Losses, Finite Element, Thermal Efficiency.**

I. INTRODUCTION

Joining of metallic parts by welding is widely used in automotive industries to assemble various products. It is well known that the welding process relies on an intensely localized heat input, result of thermally induced plastic deformations, the internal stresses, namely, the welding residual stresses remain in the welded components and structures. These residual stresses are associated with the thermal cycles and develop when the components/ structures cool down to ambient temperature. Structural parameters (viz., geometry and joint type), material parameters (viz., mechanical and physical properties, and type of filler metal), and welding process parameters (viz., current, voltage, arc travel speed, arc efficiency, and type of process) do strongly affect residual stress distribution and distortion in weld joints and structures. The resulting residual stresses have a strong influence on weld deformation, fatigue, fracture, creep and buckling.

Depending on magnitude, sign (tension or compression) and the distribution of the stresses with respect to the load-induced stresses, the effect of residual stresses may either be beneficial or detrimental. Hence, it is necessary to understand the mechanism of metal deformation induced by intense heat associated with welding heat source under both the internal and external conditions.

To date, number of expensive or destructive techniques has been employed for measuring residual stresses in metals. X-ray diffraction can be used to measure residual stress at the structure surface, because the penetration depth of X-rays is extremely shallow. The principle of neutron diffraction is the same as that of X-ray diffraction. Since the penetration depth of neutrons is deep, neutron diffraction can be used to measure the through-thickness residual stress in welded structures [1-4]. Nevertheless, more traditional approaches, mainly based on the strains produced in the body as a consequence of residual stress relaxation, are still widely employed due to their satisfactory accuracy and relatively low cost [5]. Strain gauges are usually utilized for strain measurements, even if more sophisticated methods, such as holography and Moire have also been applied. Numerical calibration techniques can be applied to improve the accuracy and resolution of these methods [6, 7]. Thermal stress analysis plays an important role in evaluation of residual stress, and of distortion, as well as microstructure modeling of welded joints and structures. Heat transfer analysis provides the thermal history in the welded joints, which will be utilized in stress analysis to determine the residual stress fields.

Rosenthal developed the first classical solutions for the heat sources in 1941 and later by Rykalin and others in the 1950s to obtain transient temperature of welded plates. An extensive survey and presentation of various analytical solutions for a number of stationary and moving heat sources in semi-infinite body, thick plate, fillet joint, cylinders, sphere and cone and their application in weld-pool simulation, residual stress and distortion calculations, microstructure modeling and optimization of multi-pass welded components were performed by Nguyen [8]. These solutions are obtained with an assumption that only conduction is playing a major part in the thermal analysis of welds. In the welding process, the fusion zone (FZ) and the heat affected zone (HAZ) regions experience high temperatures, which cause phase transformations and alterations in the mechanical properties of the welded metal. The estimates of temperature distribution in multiple pass welding is more complex than in the single pass processes due to superimposed thermal effects of one pass over the previous passes. The effect of thermal cycles obtained from the distributed (Gaussian) heat source model are found to be more reliable than those obtained from the concentrated (point) heat source model [9]. The finite element method (FEM) is the overall dominant tool used for analyzing various types of welded joints [10-12].

The various issues involved in the development of material models used for residual stress analysis have been discussed in detail by Lindgren [13]. Duranton et al. [14] have computed distortions and residual stresses through the 3D finite element simulations of multi-pass welding of a 316L stainless steel. The finite element simulation of

International Journal of Electronics Communication and Computer Engineering
Volume 4, Issue 2, ISSN (Online): 2249–071X, ISSN (Print): 2278–4209

three-dimensional transient residual stresses in a Tee-joint has been performed by Murugan and Narayanan [15] and the authors used a contour method to experimentally validate the numerical results. The finite element simulation of temperature field and residual stresses of butt-welded plates have been executed over the last two decades [16-19]. The inherent strain method has been used by Ueda and Yuan [20, 21] and Mochizuki and Hattori [22] to calculate the residual stresses. Dong [23] has proposed a model utilizing the element birth and death technique to simulate the metal deposition that is valid in the case with no thermal effects of the sudden larger temperature variation. A new technique of element movement for full 3D simulation of the welding process has been introduced by Fanous et al. [24].

A 3D finite element welding simulation and predicted weld-induced residual stresses in butt welding of two similar carbon steel plates have been performed by Stamenkovic and Vasovic [25]. The welding simulation was considered as a sequentially coupled thermo-mechanical analysis and the element birth and death technique was employed for the simulation of filler metal deposition. The finite element analysis results are found to be very close to the experimental results. The thickness effect on the residual stress states in butt-welded 2.25Cr1Mo steel plates have been examined by Tahami et al. [26]. Finite element analysis results show that by increasing the plate thickness, the residual stresses increase and the residual stress affected zone becomes larger. The longitudinal residual stress in weld axis changes from compressive to tensile by increasing the plate thickness. The effect of the welding-electrode speed using birth and death of finite elements has been studied by Tahami and Sorkhabi [27]. They have shown that use of the 3D and transient model will lead to more accurate and realistic results which are well compared with the test data. Jeyakumar et al. [28] have performed a 2D finite element analysis and predicted weld-induced residual stresses in butt welded two similar 2.25 Cr1Mo low-alloy ferritic steel plates and also ASTM A36 steel plates. Accurate and reliable residual stress prediction and measurements are essential for structural integrity assessment of components containing residual stresses. Commercially available finite element method (FEM) packages such as ABAQUS, ANSYS, NASTRAN, MARC, etc. can be used for welding thermal elastic plastic stresses and distortion analyses. Finite element simulation of residual stresses due to welding involves in general many phenomena, e.g. nonlinear temperature dependent material behavior, 3D nature of weld-pool and the welding processes and micro structural phase transformation. In this paper, the finite element analysis of residual stresses in butt welding of ASTM A36 steel plates is performed utilizing the ANSYS. The present analysis results are found to be in good agreement with experiment results and the existing 2D finite element analysis.

II. WELDING SIMULATION

The thermal history of welded joints is generally predicted from heat transfer analysis. Subsequently, the calculated thermal history can be used for thermal stress analysis to determine the residual stress fields in the welded joints. Heat can be transmitted by conduction, convection and radiation during welding processes. For welding processes where an electric arc is used as the welding source, heat conduction through the metal body is the major mode of heat transfer and heat convection is less significant as far as the temperature field in the welded body is concerned. The partial differential equation for transient heat conduction is

$$\rho c \frac{\partial T}{\partial t} = \nabla.(\kappa \nabla T) + f \tag{1}$$

Where the density (ρ), specific heat (c) and the thermal conductivity (κ) are dependent on temperature (T). t is the time and f represents the additional heat-generation function in the body.

$$c = \frac{dH}{dT} \tag{2}$$

From Eqs. (1) and (2), one can write the apparent heat capacity equation in the form

$$\rho \frac{\partial H}{\partial t} = \nabla.(\kappa \nabla T) + f \tag{3}$$

The problem to be solved is defined by the heat conduction equation together with initial and boundary conditions. Simple boundary conditions are prescribed temperature or prescribed heat flux. The surface heat flux, q_n is defined as positive when directed in the outward normal direction. It is zero in the case of an isolated, adiabatic boundary. Convective and radiation heat losses are more complex boundary conditions for the outward flux. Then the surface heat flux depends on the temperature of the body and the surrounding and is written as

$$q_n = -\kappa \nabla T.\vec{n} = -\kappa \frac{\partial T}{\partial n} = h_c (T - T_{ref}) + e_f s_b (T^4 - T_{ref}^4) \tag{4}$$

Where the first term is convective heat loss and h_c is the heat transfer coefficient. The second term is the heat loss due to radiation and s_b is Stefan-Bolzmann's constant and e_f is the emissivity factor. The second term is a nonlinear boundary condition. The total heat loss in Eq. (4) can be written in a format more convenient for finite element implementation as

$$q_n = \{h_c + e_f s_b (T^2 + T_{ref}^2)(T + T_{ref})\}(T - T_{ref}) = h_{eff}(T - T_{ref}) \tag{5}$$

The effective heat transfer coefficient (h_{eff}) is a combination of both the convection and radiation coefficients:

$$h_{eff} = h_c + e_f s_b (T^3 + T^2 T_{ref} + T T_{ref}^2 + T_{ref}^3) \tag{6}$$

Heat input is the most important parameter to determine the temperature distribution in the welded components. This heat quantity is the output from a particular heat

source used to fabricate the welded joints. Heat source provides the required energy and causes localized high temperature spot, in all the welding processes. In arc-welding with constant voltage (*V*) and amperage (*I*), the efficiency of the heat source would be

$$\eta = \frac{Q_S\, t_{weld}}{V\, I\, t_{weld}} = \frac{Q_S}{V\, I} \tag{7}$$

Where Q_S is the heat generating rate and t_{weld} is the welding time and η is the thermal efficiency. The Gaussian-distributed volumetric heat source can be used to simulate the welding to give a better prediction of the temperature field near the source center. The Gaussian volumetric heat source is used to simulate the welding-arc, where the heat source density, *q(x, y, z)* at an arbitrary point *(x, y, z)* is represented by [8]

$$q(r) = \frac{3\sqrt{3}\,Q}{\pi\sqrt{\pi}\,r_b^3} e^{-3(r/r_b)^2} \tag{8}$$

The distance *r* in Eq. (8) is the distance from the center point of the heat source to the point for which the heat generation is being calculated.

The distribution of *q(x, y, z)* in Eq. (8) represents 95% of the total heat *Q* when applied within a sphere with radius r_b. The distance, $r = \sqrt{(x - x_h)^2 + y^2 + z^2}$; $x_h = v(t - t_0)$ and *v* is the welding speed.

The calculation of welding residual stresses is usually based on the temperature distribution and the thermal stress increment $\Delta\sigma$ $(= E\alpha\Delta T)$ is calculated from the incremental thermal strain $\alpha\Delta T$. Here α is the thermal expansion and *E* is the Young's modulus. The residual stresses arise not only from the welding shrinkage but also from the surface quenching (rapid cooling of the weld surface layers) and phase transformation (transformation of austenite during the cooling cycle).

The calculation starts with time *t=0* and the thermal stress is calculated for the initial temperature distribution of the welded components. At the next time step, the thermal stress increment is added to the initial stress at step *t=0*. The magnitude of the cumulative thermal stress is limited to the yield strength of the material at actual temperatures. It should be noted that at each step, the forces caused by the induced thermal stresses must be in equilibrium. This procedure is repeated until the last step at which the thermal stress is that at ambient temperature, i.e. the residual stress.

III. Butt-Welded Steel Plates

Residual stress analysis has been carried out in a butt-weld joint of ASTM A36 steel plate (200 x 100 x 3mm) as shown in Fig.1 is examined.

Table 1 gives the temperature dependent properties. The commercial finite element code ANSYS has been used to carry out the thermal and mechanical analyses.

In order to perform the thermal analysis, 3D element SOLID70 is used. The element has eight nodes with a single degree of freedom, temperature, at each node. The FE model contains 25755 nodes and 20000 elements. The temperature dependent thermal material properties for the plates, heat affected zone and the filler weld material were assumed to be the same. The material deposition is modeled using an element "birth and death" technique. To achieve the "death element" effect, the ANSYS code does not actually remove the element from the model. Instead, the weld elements are first deactivated by multiplying their stiffness by a huge reduction factor. Meanwhile, to obtain the "birth element" effect, the ANSYS program then reactivates the "death element" by allowing its stiffness, mass, element loads, etc return to their original values.

Temperature around the arc is generally higher than the melting temperature of materials and drops sharply in regions away from weld pool. In high temperature gradient regions of FZ and HAZ, more refined mesh close to weld line is essential for obtaining accurate temperature field.

The overall input of heat flux *Q* is evaluated from Eq. (8) specifying the arc efficiency, η=0.85; arc voltage, *V*=24V; and the current, *I*=180A. In the present analysis, r_b is set to 3 mm. Welding speed = 5 mm/sec. The heat source is assumed to move through volume and calculated heat is applied to elements as volumetric heat generation.

The thermal analysis is straight forward compared with the mechanical analysis. The mechanical properties are more difficult to obtain than the thermal properties, especially at high temperatures, and they contribute to the numerical problems in the solution process [7, 20]. Many analyses use a cut-off temperature above which no changes in the mechanical properties are accounted for [21]. It serves as an upper limit of the temperature in the mechanical analysis. Tekriwal and Mazumder [29] varied the cut-off temperature up to the melting temperature. The residual transverse stress was overestimated by 2-15% when the cut-off temperature was lowered. It should be noted that all material models need to have good thermo-elasto-plastic properties up to the cut-off temperature.

It is assumed that the filler weld material has the same chemical composition of the parent material. The melting temperature of the filler material is 1783K. A cut-off temperature ($T_{cut\text{-}off}$) is set to 1073K. The material properties at $T_{cut\text{-}off}$ are specified in the regions where the temperature is higher than $T_{cut\text{-}off}$. For convective and radiative heat losses, the constants in the complex boundary conditions for the outward flux in Eq. (6) are: Stefan-Boltzmann constant, $S_b = 5.67X10^{-8} W/m^2K^4$; convection coefficient, $h_c = 15\,W/m^2K$; and the emissivity factor, e_f =0.2.

To obtain thermal history, transient, non–linear thermal problem is solved using temperature dependent thermal properties and considering heat conduction, convective and radiative boundary conditions. In thermal analysis the heat source is specified in 3082 time steps. It takes 6012 seconds to cool down from the maximum temperature to ambient (room) temperature. Since load steps are too many, Ansys Parametric Design Language (APDL) has been adopted to perform both thermal and structural analyses. For structural analysis 3D element SOLID45 is

International Journal of Electronics Communication and Computer Engineering
Volume 4, Issue 2, ISSN (Online): 2249–071X, ISSN (Print): 2278–4209

used. The element is defined by eight nodes having three degrees of freedom at each node: translations in the nodal x, y, and z directions. Thermal stress analysis is performed specifying the temperature distribution, temperature dependent mechanical properties and symmetry boundary conditions to obtain the transient and residual stress fields. For the mechanical material properties, same material models were used for the weld beads and the base materials according to the yield strength.

IV. Results and Discussion

The temperature variation from the weld center line to the edge of the plate along Y-direction (that is along the length of the plate) is shown in Fig. 2. The peak temperature reaches up to 1973K for the present analysis and 2112K in 2D FEA [28], are in good agreement. The results indicate that the plate is undergoing significant temperature variation. At the beginning, the temperature reduction in the area close to the weld axis shows the quenching effect. Fig. 3 shows the residual stress (σ_x) distribution along top, middle and bottom surfaces perpendicular to the weld obtained from the present analysis, and it is compared with experiment result [25] and 2D finite element analysis [28] . The analysis result varies from 383 MPa (tensile) to -78 MPa (compressive) and reaches to zero at top surface, while it varies from 380.8 MPa (tensile) to -77.5 MPa (compressive) and reaches to zero at middle surface, also varies from 388.4 MPa (tensile) to -99 MPa (compressive) and reaches to zero at bottom surface, while it varies from 380.5 MPa (tensile) to -190 MPa (compressive) and reaches to zero in experiment and from 389 MPa (tensile) to -132 MPa (compressive) and reaches to zero in 2D FEA results, is in good agreement.

Fig. 4 shows the residual stress (σ_x) distribution along top, middle and bottom surfaces along the weld line obtained from the present analysis, and is compared with 2D finite element analysis results [28]. The analysis result varies from 386 MPa (tensile) to -272 MPa (compressive) at top surface, while it varies from 394 MPa (tensile) to -132 MPa (compressive) at middle surface, also varies from 385.6 MPa (tensile) to -131.4 MPa (compressive) at bottom surface while it varies from 387 MPa (tensile) to -1 MPa (compressive) in 2D FEA results.

Fig. 5 illustrates the residual stress (σ_y) distribution for top, middle and bottom surfaces along the weld line obtained from the present analysis and is compared with 2D finite element analysis results [28]. The analysis result varies from 80 MPa (tensile) to -543 MPa (compressive), while it varies from 108 MPa (tensile) to -497 MPa (compressive) at middle surface, also varies from 83.5 MPa (tensile) to -434 MPa (compressive) at bottom surface, while it varies from 161 MPa (tensile) to -343 MPa (compressive) in 2D FEA results, is in good agreement. Fig. 6 shows the residual stress (σ_x) distribution through thickness at weld center line. The result varies from 388 MPa to 384 Mpa (tensile). Fig. 7 depicts the residual stress (σ_y) distribution through thickness at weld center line. The result varies from 72.5 MPa to 50.8 Mpa (tensile). Table 2 gives the values of residual stresses at mid section of the plate perpendicular to weld. The values of residual strains at mid section of the plate perpendicular to weld are enumerated in Table 3. Table 4 details the values of residual stresses along weld line.

V. Concluding Remarks

3D Finite element analysis has been carried out utilizing the commercial software package ANSYS to estimate the temperature distribution and residual stresses in the butt-welded ASTM A36 steel plates. The distribution of residual stresses and strains along top, middle and bottom surfaces perpendicular to the weld and along weld line are obtained from the present analysis, and is compared with experiment result [25] and 2D finite element analysis [28], is in good agreement.

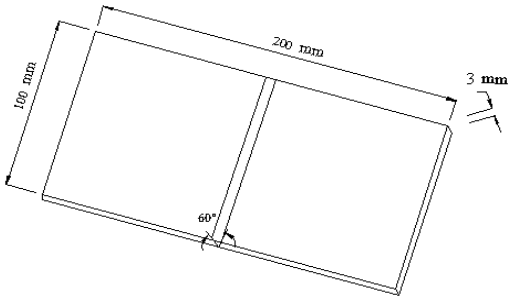

Fig.1. Butt-welded steel plates

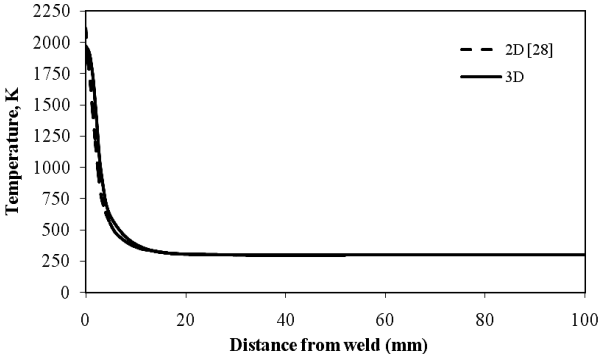

Fig.2. Comparison of Temperature distribution at 10 sec

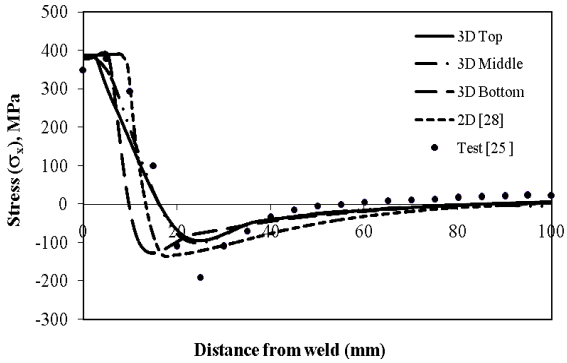

Fig.3. Comparison of Residual stress, σ_x from the weld center line to the edge of the plate along its transverse direction

International Journal of Electronics Communication and Computer Engineering
Volume 4, Issue 2, ISSN (Online): 2249–071X, ISSN (Print): 2278–4209

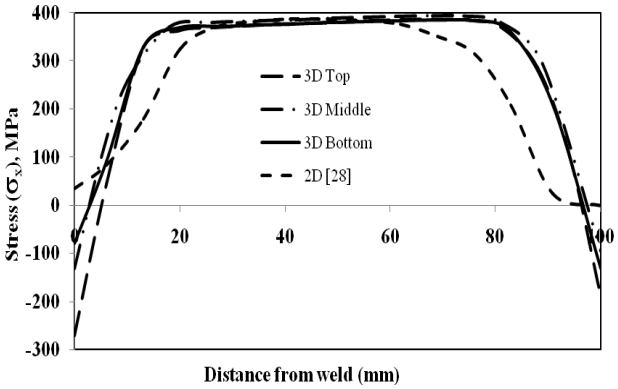

Fig.4. Comparison of Residual stress, σ_x along weld line

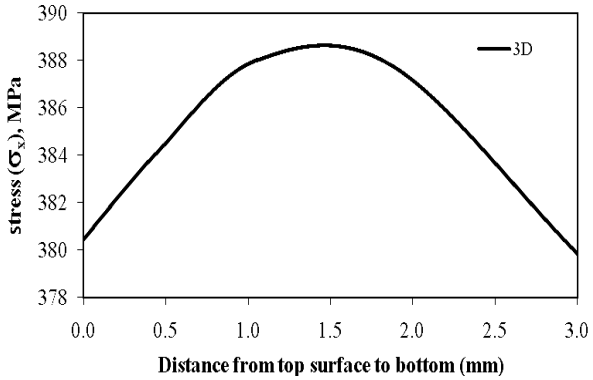

Fig.6. Through thickness distribution of Residual stress, σ_x at weld center line

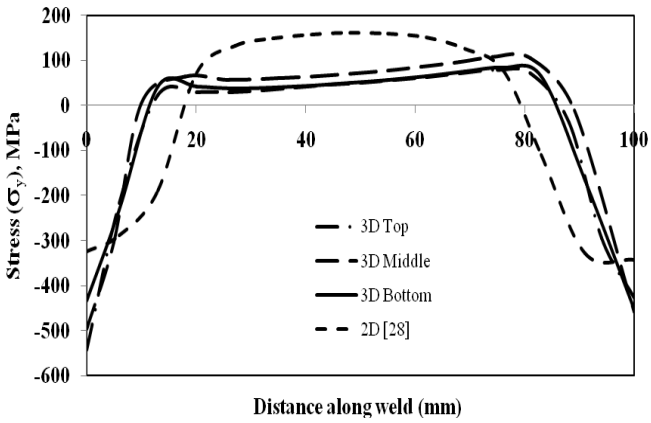

Fig.5. Comparison of Residual stress, σ_y along weld line

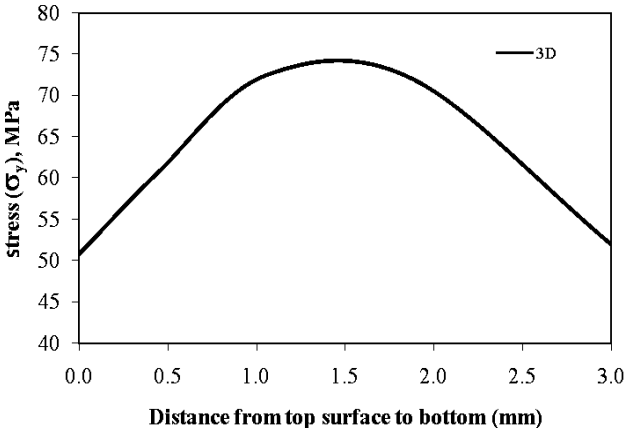

Fig.7. Through thickness distribution of Residual stress, σ_y at weld center line

Table 1: Variation of physical properties of the material with temperature [28]

Chemical Composition (%wt)				
C	Mn	P	S	Si
0.28	0.60~0.90	0.04	0.05	0.40

Temp (K)	**Density (Kg/m^3)**	**Elastic modulus (GPa)**	**Poisson's ratio**	**Thermal expansion Coefficient (K^{-1})X10^{-5}**	**Thermal conductivity W/(m-K)**	**Specific heat (J/(Kg-K))**	**Yield stress (MPa)**
298	7880	210	0.3	1.15	60	480	380
373	7880	200	0.3	1.2	50	500	340
473	7800	200	0.3	1.3	45	520	315
673	7760	170	0.3	1.42	38	650	230
873	7600	80	0.3	1.45	30	750	110
1073	7520	35	0.3	1.45	25	1000	30
1273	7390	20	0.3	1.45	26	1200	25
1473	7300	15	0.3	1.45	28	1400	20
1673	7250	10	0.3	1.45	37	1600	18
1773	7180	10	0.3	1.45	37	1700	15

Table 2: Residual Stresses at mid section of the plate perpendicular to weld

Distance from weld line (mm)	Top Surface (MPa)			Middle Surface (MPa)			Bottom Surface (MPa)		
	σ_x	σ_y	σ_{eff}	σ_x	σ_y	σ_{eff}	σ_x	σ_y	σ_{eff}
0.0	380.5	50.8	358.5	378.5	46.0	358.3	379.8	52.0	357.2
1.0	380.4	49.2	358.3	378.3	44.0	358.2	380.8	53.8	357.1
2.6	383.1	52.9	358.0	380.8	47.5	357.8	382.9	56.2	357.0
6.7	255.7	94.2	223.8	329.6	104.0	292.2	388.4	98.3	354.3
20.8	-77.8	46.9	109.9	-77.5	42.2	114.0	-99.0	59.1	138.6
37.0	-46.2	20.0	59.3	-44.7	17.1	58.2	-76.4	40.3	103.1
52.0	-22.9	5.7	26.5	-21.9	44.0	25.5	-35.0	10.8	41.7
77.2	-3.1	-0.5	3.0	-2.9	-0.7	2.9	-7.4	-0.1	7.4
100.0	6.6	-0.1	6.7	-6.6	-0.1	6.6	5.3	0.0	5.3

Table 3: Residual Strains at mid section of the plate perpendicular to weld

Distance from weld line (mm)	Top Surface			Middle Surface			Bottom Surface		
	ε_x	ε_y	ε_{eff}	ε_x	ε_y	ε_{eff}	ε_x	ε_y	ε_{eff}
0.0	-0.0006	-0.0233	0.0297	-0.0006	-0.0230	0.0294	-0.0006	-0.0398	0.0487
1.0	-0.0006	-0.0287	0.0000	-0.0007	-0.0283	0.0520	-0.0007	-0.0406	0.0520
2.6	-0.0006	-0.0139	0.0373	-0.0006	-0.0137	0.0225	-0.0006	-0.0122	0.0216
6.7	-0.0005	0.0006	0.0226	-0.0005	0.0006	0.0027	-0.0005	0.0003	0.0043
20.8	-0.0004	0.0003	0.0028	-0.0006	0.0003	0.0005	-0.0006	0.0004	0.0007
37.0	-0.0002	0.0002	0.0005	-0.0004	0.0002	0.0003	-0.0004	0.0003	0.0005
52.0	-0.0001	0.0001	0.0003	-0.0002	0.0000	0.0001	-0.0002	0.0001	0.0002
77.2	0.0000	0.0000	0.0001	0.0000	0.0000	0.0000	0.0000	0.0000	0.0000
100.0	0.0000	0.0000	0.0000	0.0000	0.0000	0.0000	0.0000	0.0000	0.0000

Table 4: Residual stresses along weld line

Distance along weld line (mm)	Top Surface (MPa)		Middle Surface (MPa)		Bottom Surface (MPa)	
	σ_x	σ_y	σ_x	σ_y	σ_x	σ_y
0	-271.8	-543.7	-132.0	-497.0	-80.1	-433.6
6	43.1	-216.4	100.0	-302.0	90.1	-232.0
13	326.9	22.7	259.0	5.0	328.6	41.1
20	363.6	29.5	370.0	64.0	368.7	42.0
27	368.8	30.2	379.0	57.0	371.5	37.3
34	372.2	34.5	383.0	60.0	374.2	40.4
41	375.3	39.8	385.0	66.0	376.8	45.1
48	378.2	45.4	388.0	72.0	379.2	50.4
55	380.5	50.8	390.0	78.0	381.4	56.5
62	382.7	56.9	392.0	86.0	383.8	64.8
69	384.8	64.1	394.0	97.0	385.6	75.1
76	386.3	72.3	393.0	108.0	383.6	83.5
83	384.5	79.5	379.0	105.0	359.9	64.4
91	108.8	-293.9	293.0	-11.0	208.9	-165.5
100	-189.4	-427.4	-96.0	-459.0	-131.4	-452.2

REFERENCES

[1] A.J. Allen, M.T. Hutchings, C.G. Windsor and C. Andreani, "Neutron diffraction methods for the study of residual stress fields", *Advances in Physics*, Vol.34, pp.445-473 (1985).

[2] M.T. Hutchings, "Neutron diffraction measurement of residual stress fields. The answer to the engineers prayer", *Journal of Nondestructive Testing and Evaluation*, Vol.5, pp.395-403 (1990).

[3] L. Wikandar, L. Karlsson, M. Nasstron and P. Webster, "Finite element simulation and measurement of welding residual stresses", *Modeling and Simulation in Materials Science and Engineering*, Vol.2, pp.845-864 (1994).

[4] M. Mochizuki, M. Hayashi and T. Hattori, "Numerical analysis of welding residual stress and its verification using neutron diffraction measurement", *Trans ASME Journal of Engineering Materials and Technology*, Vol.122, pp.98-103 (2000).

[5] M. Beghini and L. Bertini, "Residual stress modeling by experimental measurements and finite element analysis", *Journal of Strain Analysis*, Vol.25, No.2, pp.103-108 (1990).

[6] D. Ritchie and R.H. Leggatt, "The measurements of the distribution of residual stress through the thickness of a welded joint", *Strain*, Vol.24, pp.61-70 (1987).

[7] G.S. Schajer, "Measurement of non-uniform residual stresses using the hole-drilling method. Parts I and II", *Trans ASME Journal of Engineering Materials and Technology*, Vol.110, pp.338-349 (1988).

[8] N.T. Nguyen, "Thermal Analysis of Welds", *WIT Press*, Southampton, UK (2004).

[9] R.N.S. Fassani and O.V. Trevisan, "Analytical modeling of multipass welding process with distributed heat source", *Journal of Brazilian Society of Mechanical Sciences and Engineering*, Vol.25, No.3, pp.302-305 (2003).

[10] H. Cerjak and H.K.D.H. Bhadeshia, "Mathematical Modelling of Welded Phenomena 3", *The Institute of Materials* (1998).

[11] D. Radaj, "Heat Effects of Welding Temperature Field, Residual Stress, Distortion", *Springer-Verlag*, Berlin (1992).

[12] D. Radaj, "Welding Residual Stresses and Distortion", *Springer-Verlag*, Berlin (2003).

[13] L.E. Lindgren, "Finite element modeling and simulation of welding, Part 2: Improved material modeling", *Journal of Thermal Stresses*, Vol.24, pp.195-231 (2001).

[14] P. Duranton, J. Devaux, V. Robin, P. Gilles and J.M. Bergheau, "3D modeling of multipass welding of a 316L stainless steel pipe", *Journal of Materials Processing Technology*, Vol.153-154, pp.457-463 (2004).

[15] N. Murugan and R. Narayanan, "Finite element simulation of residual stresses and their measurement by contour method", *Materials and Design*, Vol.30, pp.2067-2071 (2009).

[16] J.A. Goldak, A. Chakravarti and M. Bibby, "A new finite element model for welding heat sources", *Metallurgical Transactions B*, Vol.15, pp.299-305 (1984).

[17] D. Deng and H. Murakawa, "Numerical simulation of temperature field and residual stress in multipass welds in stainless steel pipe and comparison with experimental measurements", *Computational Materials Science*, Vol.37, pp.269-277 (2006).

[18] W. Jiang, K. Yahiaoui and F.R. Hall, "Finite element predictions of temperature distributions in a multipass welded piping branch junction", *Trans ASME Journal of Pressure Vessel Technology*, Vol.127, pp.7-12 (2005).

[19] M. Iranmanesh and A.R. Darvazi, "Analytical and numerical simulation of temperature field and residual stresses of butt weld in steel plates used in ship manufacturing", *Asian Journal of Applied Sciences*, Vol.1, pp.70-78 (2008).

[20] Y. Ueda and M.G. Yuan, "Prediction of residual stresses in butt welded plates using inherent strains", *Trans ASME Journal of Engineering Materials and Technology*, Vol.115, pp.417-423 (1993).

[21] Y. Ueda and M.G. Yuan, "Prediction of residual stresses in welded T- and I-joints using inherent strains", *Trans ASME Journal of Engineering Materials and Technology*, Vol.118, pp.229-234 (1996).

[22] H. Mochizuki and H. Hattori, "Residual stress analysis by simplified inherent strains at welded pipe junctions in a pressure vessel", *Trans ASME Journal of Pressure Vessel Technology*, Vol.121, pp.353-357 (1999).

[23] P. Dong, "Residual stress analysis of multipass birth weld: #D special shell versus axisymmetric models", *Trans ASME Journal of Pressure Vessel Technology*, Vol.123, pp.207-213 (2001).

[24] I.F.Z. Fanous, M.Y.A. Younan and A.S. Wifi, "3D finite element modeling of the welding process using element birth and element movement techniques", *Trans ASME Journal of Pressure Vessel Technology*, Vol.125, pp.144-150 (2003).

[25] D. Stamenkovic and I. Vasovic, "Finite element anaysis of residual stress in butt welding two similar plates", *Scientific Technical Reviews*, Vol.59, pp.57-60 (2009).

[26] F.V. Tahami, A.H.D. Sorkhabi, M.A. Saeimis and A. Homayounfar, "3D finite element analysis of the residual stresses in butt-welded plates with modeling of the electrode-movement", *Journal of Zhejiang University Science A*, Vol.10, pp.37-43 (2009).

[27] F.V. Tahami and A.H.D. Sorkhabi, "Finite element analysis of thickness effect on the residual stress in butt-welded 2.25Cr1Mo steel plates", *Journal of Applied Sciences*, Vol.9, pp.1331-1337 (2009).

[28] M. Jeyakumar, T. Christopher, R. Narayanan & B. Nageswara Rao, "Residual stress evaluation in butt-welded steel plates", *Indian Journal Engineering and Material Sciences*, Vol.18, pp.425-434(2011)

[29] P. Tekriwal and J. Mazumder, "Transient and residual thermal strain-stress analysis of GMAW", *Trans ASME Journal of Engineering Materials and Technology*, Vol.113, pp.336-343 (1991).

AUTHOR'S PROFILE

M. Jeyakumar

Obtained his B.E (Mechanical Engineering) from M.S University, Tirunelveli, and M.E (Production Engineering) from M.K. University, Madurai, India. He is a Professor/ Head of Mechanical Engineering Department and Principal, Sardar Raja College of Engineering, Alangulam, Tamilnadu, India. His current research areas include Finite Element Analysis, Fracture Mechanics, Material Science and Welding.

T. Christopher

He is a Professor and Head of Mechanical Engineering Department, Government College of Engineering, Tirunelveli, Tamilnadu, India. He has been a committee member for various International and National conferences. He has 20 research publications at International/National Journals and Conferences. His areas of interest include Elasto-plastic behaviour of materials, Fracture Mechanics, Finite Element Analysis, Welding and Material Science.

B. Nageswara Rao

Obtained his M.Sc. (1975) and Ph.D. (1982) in Mathematics from Indian Institute of Technology, Bombay and worked as a Scientist (1979 - 2012) in Vikram Sarabhai Space Centre, Trivandrum. After superannuation from Govt. service, he is currently working as a Professor in the Department of Mechanical Engineering, KL University, Green Fields, Vaddeswaram. His areas of interest include Boundary Layer Flows, Fracture Mechanics, Hot and Cold Working Characteristics of Materials and Rocket motor cases/ Pressure Vessels. He has contributed 260 articles to international journals, 20 articles to national journals and 40 papers to national/international conferences.